Heat and Mass Transfer 38 (2002) 487–495 © Springer-Verlag 2001
DOI 10.1007/s002310100269

Combined heat and mass transfer by hydromagnetic natural convection over a cone embedded in a non-Darcian porous medium with heat generation/absorption effects

Ali J. Chamkha, Mir Mujtaba A. Quadri

Abstract The problem of combined heat and mass transfer by natural convection over a permeable cone embedded in a uniform porous medium in the presence of an external magnetic field and internal heat generation or absorption effects is formulated. The cone surface is maintained at either constant temperature and constant concentration or uniform heat and mass fluxes. In addition, the cone surface is assumed permeable in order to allow for possible fluid wall suction or blowing. The resulting governing equations are non-dimensionalized and transformed into a non-similar form and then solved numerically by an implicit, iterative, finite-difference method. Comparisons with previously published work are performed and excellent agreement between the results is obtained. A parametric study of the physical parameters is conducted and a representative set of numerical results for the temperature and concentration profiles as well as the local Nusselt number and the Sherwood number is illustrated graphically to show special trends of the solutions.

List of symbols

B_o	magnetic induction
c	concentration
C	dimensionless concentration, $(c - c_\infty)/(c_w - c_\infty)$ for (UWT/UWC) case
C	dimensionless concentration, $(c - c_\infty)D(\mathrm{Ra}_x^*)^{1/3}/(m_w x)$ for (UHF/UMF) case
C^*	porous medium inertia coefficient
D	mass diffusivity
f	dimensionless stream function, $\psi/(\alpha_e \gamma \mathrm{Ra}_x^{1/2})$ for (UWT/UWC) case
f	dimensionless stream function, $\psi/(\alpha_e \gamma \mathrm{Ra}_x^{*1/3})$ for (UHF/UMF) case
F_r	dimensionless porous medium inertia parameter, $C^* K \alpha_e \mathrm{Ra}_x/(\nu x)$ for (UWT/UWC) case
F_r^*	dimensionless porous medium inertia parameter, $C^* K \alpha_e \mathrm{Ra}_x^{*1/3}/(2\nu v_w x^{2/3})$ for (UHF/UMF) case
g	gravitational acceleration
Ha	Hartmann number, $(\sigma B_o^2 K/(\rho \nu))^{1/2}$
h	heat transfer coefficient
h_m	mass transfer coefficient
K	porous medium permeability
k_e	effective porous medium thermal conductivity
Le	Lewis number, α_e/D
m_w	wall mass flux
N	buoyancy ratio, $\beta_c(c_w - c_\infty)/[\beta_T(T_w - T_\infty)]$ for (UWT/UWC) case
N^*	buoyancy ratio, $\beta_c(m_w/D)/[\beta_T(q_w/k_e)]$ for (UHF/UMF) case
Nu_x	Nusselt Number, hx/k_e
q_w	wall heat flux
Q_o	heat generation or absorption coefficient
Ra_x	local modified Rayleigh number, $g\beta_T K \cos(\gamma)(T_w - T_\infty)x/(\nu\alpha_e)$ for (UWT/UWC) case
Ra_x^*	local modified Rayleigh number, $g\beta_T K q_w x^2 \cos(\gamma)/(\nu\alpha_e k_e)$ for (UHF/UMF) case
Sh_x	local sherwood number, $h_m x/D$
T	temperature
UWT/UWC	uniform wall temperature/uniform wall concentration
UHF/UMF	uniform heat flux/uniform mass flux
u	velocity in the x-direction
v	velocity in the y-direction
v_w	suction or injection velocity
x	streamwise coordinate
y	transverse coordinate

Greek symbols

α_e	effective porous medium thermal diffusivity
β_c	coefficient of concentration expansion
β_T	coefficient of thermal expansion
δ	dimensionless heat generation or absorption coefficient, $Q_o \alpha_e/(4\rho c_p v_w^2)$
η	pseudo-similarity variable, $y\mathrm{Ra}_x^{1/2}/x$ for (UWT/UWC) case
η	pseudo-similarity variable, $y\mathrm{Ra}_x^{*1/3}/x$ for (UWT/UWC) case
γ	cone half angle
θ	dimensionless temperature, $(T - T_\infty)/(T_w - T_\infty)$ for (UWT/UWC) case
θ	dimensionless temperature, $(T - T_\infty)k_e(\mathrm{Ra}_x^*)^{1/3}/(q_w x)$ for (UHF/UMF) case
ν	kinematic viscosity
σ	electrical conductivity

Received on 5 June 2000 / Published online: 29 November 2001

Ali J. Chamkha (✉), Mir Mujtaba A. Quadri
Department of Mechanical and Industrial Engineering
Kuwait University P.O. Box 5969, Safat, 13060 – Kuwait

ξ	dimensionless coordinate, $2\nu_w x/(\alpha_e \mathrm{Ra}_x^{1/2})$ for (UWT/UWC) case
ξ	dimensionless coordinate, $2\nu_w x/(\alpha_e \mathrm{Ra}_x^{*1/3})$ for (UHF/UMF) case
ψ	stream function

Subscripts

w	condition at the wall
∞	condition at free stream

1 Introduction

Combined heat and mass transfer (or double-diffusion) in fluid-saturated porous media finds applications in a variety of engineering processes such as heat exchanger devices, petroleum reservoirs, chemical catalytic reactors and processes, geothermal and geophysical engineering such as moisture migration in fibrous insulation and nuclear waste disposal and others. Double diffusive flow is driven by buoyancy due to temperature and concentration gradients. There have been considerable work done on the study of flow and heat transfer in various geometries embedded in porous media (see for instance, Nield and Bejan [1] and Trevisan and Bejan [2]).

The Darcy law has been employed extensively in many investigations on porous media. It is valid for slow flows and does not account for inertia effects and the presence of a boundary. For example, the problem of natural convection in a porous medium supported by an isothermal vertical plate was solved some time ago by Cheng and Minkowycz [3] using the Darcy law. It is well established now that the Darcy law is inadequate for modeling high velocity flow situations for which the pressure drop is a quadratic function of the flow rate. Johnson and Cheng [4], Vafai and Tien [5] and Plumb and Huenefeld [6] were among the first to consider inertia effects in porous media.

Natural convection flow induced by buoyancy due to temperature gradient about a horizontal cylinder embedded in a porous medium has been investigated by Merkin [7] who obtained a similarity solution. Fand et al. [8] have reported experimental results and Nakayama and Koyama [9] have solved the problem using the integral method. Ingham and Pop [10] and Pop et al. [11] have reported numerical results based on the finite-difference methodology.

Recently, a significant number of investigations have been carried out on the effects of electrically-conducting fluids such as liquid metals, water mixed with a little acid, and others in the presence of a magnetic field on the flow and heat transfer aspects (for example, Sparrow and Cess [12], Gray [13], Michiyoshi, Takahashi and Serizawa [14], Fumizawa [15] and Riley [16]. Also, the study of heat generation or absorption effects in moving fluids is important in view of several physical problems, such as fluids undergoing exothermic or endothermic chemical reactions (see Vajravelu and Hadjinicolaou [17] and Vajravelu and Nayfeh [18]). In addition, Kou and Lu [19] showed that the design of placing many electronic circuits into one small chip and more chips into a package results in high volumetric heat generation in the electronic equipment. This led to the consideration of heat generation effects in porous media. In addition, recently, Chamkha [20] analyzed the problem of non-Darcy free convection flow about wedge and a cone embedded in a porous media in the presence of heat generation effects.

The coupled heat and mass transfer problem received relatively little attention. Trevisan and Bejan [2] considered combined heat and mass transfer by natural convection in a porous medium for various geometries. Bejan and Khair [21] reported on the natural convection boundary-layer flow in a saturated porous medium with combined heat and mass transfer. The coupled heat and mass buoyancy-induced inclined boundary layer in a porous medium was studied by Jang and Chang [22]. Later, Lai and Kulacki [23] extended the problem of Bejan and Khair [21] to include wall fluid injection effects. Yucel [24] has considered coupled heat and mass transfer about a vertical cylinder in porous media. Lai and Kulacki [25] have investigated coupled heat and mass transfer by natural convection from a sphere embedded in porous media. Yih [26] has considered coupled heat and mass transfer by natural convection adjacent to a permeable horizontal cylinder in a saturated porous medium. Recently, Yih [27] has reported on uniform transpiration effect on combined heat and mass transfer by natural convection over a cone in saturated porous media for the cases of uniform wall temperature/concentration and uniform wall heat/mass fluxes.

The purpose of the present work is to extend the work of Yih [27] by including such effects as porous medium inertia, magnetic field, and heat generation or an absorption effects. This is motivated by applications such as petroleum prospecting and production and detection of groundwater contamination and metalurgical applications in the presence of a magnetic field.

2 Governing equations

Consider combined heat and mass transfer by hydromagnetic natural convection over a permeable cone embedded in a uniform porous medium in the presence of heat generation or absorption effects. A uniform magnetic field is applied in the direction normal to the cone surface. The surface of the cone is maintained at uniform temperature T_w and uniform concentration c_w or uniform heat flux q_w and uniform mass flux m_w. Far from the cone surface, the free stream is kept at a constant temperature T_∞ and a constant concentration c_∞. Constant fluid suction or injection is imposed at the surface of the cone (Fig. 1). The fluid is assumed to be Newtonian, viscous, heat generating or absorbing and electrically conducting. The surface of the cone and the porous medium are assumed to be electrically insulating and are in local thermal equilibrium. All fluid properties are assumed constant except the density in the buoyancy term of the x-momentum equation. The magnetic Reynolds number is assumed small so that the induced magnetic field is neglected. In addition, no electric field is assumed to exist and the Hall effect is negligible. In the absence of an electric field, the small magnetic Reynolds number assumption uncouples Maxwell's equations from the Navier–Stokes equations (Cramer and Pai [28]). Taking all of the above assumptions into consideration and invoking

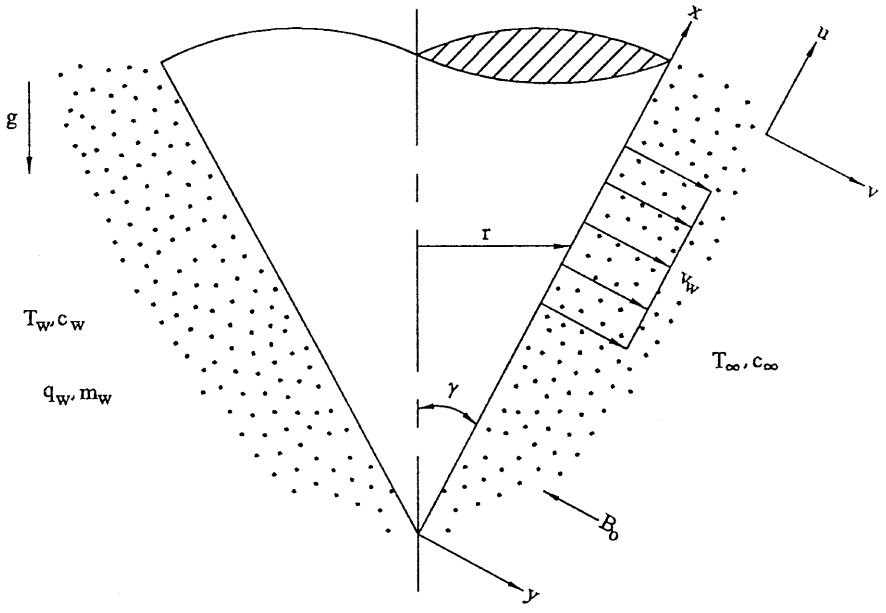

Fig. 1. Flow model and physical coordinate system

the boundary-layer and Boussinesq approximations, the governing equations based on the modified Darcy law which includes the porous medium inertia effects can be written as

$$\frac{\partial(ru)}{\partial x}+\frac{\partial(rv)}{\partial y}=0 \tag{1}$$

$$\left(1+\frac{\sigma B_o^2 K}{\rho\nu}+\frac{2C^* K}{\nu}u\right)\frac{\partial u}{\partial y}=\frac{Kg}{\nu}\cos(\gamma)\left[\beta_T\frac{\partial T}{\partial y}+\beta_c\frac{\partial c}{\partial y}\right] \tag{2}$$

$$u\frac{\partial T}{\partial x}+v\frac{\partial T}{\partial y}=\alpha_e\frac{\partial^2 T}{\partial y^2}+\frac{Q_o}{\rho c_p}(T-T_\infty) \tag{3}$$

$$u\frac{\partial c}{\partial x}+v\frac{\partial c}{\partial y}=D\frac{\partial^2 c}{\partial y^2} \tag{4}$$

where r is the cone radius and x and y are the circumferential or streamwise and the transverse distances, respectively. u, v, T and c are the fluid x-component of velocity, y-component of velocity, temperature, and concentration, respectively. ρ, ν, c_p, β_T and β_c are the fluid density, kinematic viscosity, specific heat at constant pressure, coefficient of thermal expansion and coefficient of concentration of expansion, respectively. K, C^* and α_e are the porous medium permeability, inertia coefficient and effective thermal diffisuvity, respectively. σ, B_o, Q_o and D are the electrical conductivity, magnetic induction, heat generation (>0) or absorption (<0) coefficient and mass diffusivity, respectively. g and γ are the acceleration due to gravity and the cone half angle.

The boundary conditions for the uniform temperature-uniform concentration case of this problem are given by

$$\begin{aligned} &y=0: v=v_w, \quad T=T_w, \quad c=c_w \\ &y\to\infty: u=0, \quad T=T_\infty, \quad c=c_\infty \end{aligned} \tag{5a–f}$$

where v_w is the suction (<0) or injection (>0) velocity.

If the uniform wall heat and mass fluxes are prescribed, Eqs. (5b) and (c) are replaced by

$$y=0: -k_e\left(\frac{\partial T}{\partial y}\right)=q_w, \quad -D\left(\frac{\partial c}{\partial y}\right)=m_w \tag{5g, h}$$

where k_e is the effective thermal conductivity of the porous medium.

2.1
Case 1: uniform wall temperature/uniform wall concentration (UWT/UWC)

For this situation, it is convenient to transform Eqs. (1) through (5a–f) by using the following non-similarity transformations reported earlier by Yih [27].

$$\begin{aligned} &\xi=\frac{2v_w x}{\alpha_e \mathrm{Ra}_x^{1/2}}, \quad \eta=\frac{y}{x}\mathrm{Ra}_x^{1/2}, \quad \psi=\alpha_e r \mathrm{Ra}_x^{1/2} f(\xi,\eta) \\ &\theta(\xi,\eta)=\frac{T-T_\infty}{T_w-T_\infty}, \quad C(\xi,\eta)=\frac{c-c_\infty}{c_w-c_\infty} \end{aligned} \tag{6}$$

where $\mathrm{Ra}_x=g\beta_T K\cos(\gamma)(T_w-T_\infty)x/(\nu\alpha_e)$ is the local modified Rayleigh number and ψ is the dimensional stream function defined by the usual way as $u=\partial\psi/\partial y$ and $v=-\partial\psi/\partial x$. In terms of the above variables, Eqs. (1) through (5a–f) become

$$(1+\mathrm{Ha}^2+2F_r f')f''=\theta'+NC' \tag{7}$$

$$\theta''+\frac{3}{2}f\theta'+\xi^2\delta\theta=\frac{\xi}{2}\left(f'\frac{\partial\theta}{\partial\xi}-\theta'\frac{\partial f}{\partial\xi}\right) \tag{8}$$

$$\frac{1}{\mathrm{Le}}C''+\frac{3}{2}fC'=\frac{\xi}{2}\left(f'\frac{\partial C}{\partial\xi}-C'\frac{\partial f}{\partial\xi}\right) \tag{9}$$

$$\begin{aligned} &\eta=0: f=\frac{-\xi}{4}, \quad \theta=1, \quad C=1 \\ &\eta\to\infty: \theta=0, \quad C=0 \end{aligned} \tag{10}$$

where

$$\mathrm{Ha}^2 = \frac{\sigma B_o^2 K}{\rho \nu}, \quad F_r = \frac{C^* K \alpha_e \mathrm{Ra}_x}{\nu x}, \quad N = \frac{\beta_c (c_w - c_\infty)}{\beta_T (T_w - T_\infty)}$$

$$\mathrm{Le} = \frac{\alpha_e}{D}, \quad \delta = \frac{Q_o \alpha_e}{4 \rho c_p \nu_w^2} \tag{11}$$

are the square of the Hartmann number, dimensionless porous medium inertia coefficient, buoyancy ratio, Lewis number, and dimensionless heat generation or absorption coefficient, respectively.

The local Nusselt and Sherwood numbers are important physical parameters for this type of problems. They can be computed from the following relations:

$$\mathrm{Nu}_x = \frac{hx}{k_e} = -\mathrm{Ra}_x^{1/2} \theta'(\xi, 0) \tag{12a}$$

$$\mathrm{Sh}_x = \frac{h_m x}{D} = -\mathrm{Ra}_x^{1/2} C'(\xi, 0) \tag{12b}$$

where h and h_m are the heat and mass transfer coefficients, respectively.

2.2
Case 2: uniform wall heat flux/uniform wall mass flux (UHF/UMF)

For this case, Yih [27] reported the following dimensionless variables

$$\xi = \frac{2 \nu_w x}{\alpha_e (\mathrm{Ra}_x^*)^{1/3}}, \quad \eta = \frac{y}{x} (\mathrm{Ra}_x^*)^{1/3}, \quad \psi = \alpha_e r (\mathrm{Ra}_x^*)^{1/3} f(\xi, \eta)$$

$$\theta(\xi, \eta) = \frac{(T - T_\infty) k_e (\mathrm{Ra}_x^*)^{1/3}}{q_w x},$$

$$C(\xi, \eta) = \frac{(C - C_\infty) D (\mathrm{Ra}_x^*)^{1/3}}{m_w x} \tag{13}$$

where $\mathrm{Ra}_x^* = g \beta_T K q_w x^2 \cos(\gamma) / (\nu \alpha_e k_e)$ is the local modified Rayleigh number.

Substitution of Eqs. (13) into Eqs. (1) through (4) and (5a, d–h) yields the following non-similar dimensionless equations:

$$(1 + \mathrm{Ha}^2 + 2\xi F_r^* f') f'' = \theta' + N^* C' \tag{14}$$

$$\theta'' + \frac{5}{3} f \theta' - \frac{1}{3} f' \theta + \xi^2 \delta \theta = \frac{\xi}{3} \left(f' \frac{\partial \theta}{\partial \xi} - \theta' \frac{\partial f}{\partial \xi} \right) \tag{15}$$

$$\frac{1}{\mathrm{Le}} C'' + \frac{5}{3} f C' - \frac{1}{3} f' C = \frac{\xi}{3} \left(f' \frac{\partial C}{\partial \xi} - C' \frac{\partial f}{\partial \xi} \right) \tag{16}$$

$$\eta = 0: \quad f = -\frac{\xi}{4}, \quad \theta' = -1, \quad C' = -1$$
$$\eta \to \infty: \ \theta = 0, \quad C = 0 \tag{17}$$

where

$$\mathrm{Ha}^2 = \frac{\sigma B_0^2 K}{\rho \nu}, \quad F_r^* = \frac{C^* K \alpha_e \mathrm{Ra}_x^{*1/3}}{2 \nu \nu_w x^{2/3}}, \quad N^* = \frac{\beta_c m_w / D}{\beta_T q_w / k_e}$$

$$\mathrm{Le} = \frac{\alpha_e}{D}, \quad \delta = \frac{Q_o \alpha_e}{4 \rho c_p \nu_w^2} \tag{18}$$

are the square of the Hartmann number, dimensionless porous medium inertia coefficient, buoyancy ratio, Lewis number and the dimensionless heat generation or absorption for this case, respectively.

The local Nusselt and Sherwood numbers for this case are given by

$$\mathrm{Nu}_x = \frac{(\mathrm{Ra}_x^*)^{1/3}}{\theta(\xi, 0)}, \quad \mathrm{Sh}_x = \frac{(\mathrm{Ra}_x^*)^{1/3}}{C(\xi, 0)} \tag{19}$$

3
Numerical method

The non-similar Eqs. (7) through (9) (or Eqs. (14) through (16)) are linearized and then descritized using three-point central difference quotients with variable step sizes in the η direction and using two-point backward difference formulae in the ξ direction with a constant step size. The resulting equations from a tri-diagonal system of algebraic equations that can be solved by the well known Thomas algorithm (see Blottmer [29]). The solution process starts at $\xi = 0$ where the equations reduce to a similar form and then marches forward (or backward) using the solution at the previous (or next) line of constant ξ until it reaches the desired value of ξ. Due to the nonlinearities of the equations, an iterative solution with successive over or under relaxation techniques is required. The solution convergence criterion required that the maximum absolute error between two successive iterations be 10^{-6} . A starting step size of 0.001 in the η direction with an increase of 1.03 times the previous step size and a constant step size in the ξ direction of 0.01 were found to give accurate results. The maximum value of η which represented the free stream conditions was assumed to be 10. This was determined by ensuring a proper asymptotic approach of both the temperature and concentration distributions to their free stream values. The accuracy of the aforementioned numerical method was validated by direct comparisons with the graphical results reported earlier by Yih [27] in the absence of magnetic field, heat generation or absorption effects. The results of these comparisons were found to be in excellent agreement.

4
Results and discussion

Figures 2 and 3 display typical temperature and concentration profiles for two different values of $\xi (\xi = -0.5$ and $\xi = 0.5)$ for various values of the Hartmann number Ha for the (UWT/UWC) case, respectively. Imposition of a magnetic field to an electrically-conducting fluid creates a drag-like force called the Lorentz force. This force has the tendency to slow down the flow along the cone surface at the expense of increasing its temperature and concentration. This is depicted by the increases in the temperature and concentration values as Ha increases shown in Figs. 2 and 3. In addition, the increases in the temperature and concentration values as Ha increases are accompanied by increases in both the thermal and concentration boundary layers. Furthermore, the effect of

fluid suction at the cone surface ($\xi = -0.5$) is seen to cause reductions in both the temperature and concentration profiles and their boundary layers. These behaviors are obvious from Figs. 2–4.

Figures 5 and 6 illustrate the behaviors of the local Nusselt and Sherwood numbers due to changes in the values of Ha, δ and ξ for the (UWT/UWC) case, respectively. For given values of δ and ξ, increasing the value of the Hartmann number causes the negative slopes of the temperature and concentration profiles at the cone surface $(-\theta'(\xi, 0)$ and $-C'(\xi, 0))$ to decrease. This has the direct effect of decreasing both the local Nusselt number and Sherwood numbers as obvious from Figs. 5 and 6. Also, for given values of Ha, increases in the values of the heat generation or absorption coefficient δ produce decreases in the values of the local Nusselt number for every value of ξ except $\xi = 0.0$. However, the local Sherwood number appears to decrease slightly for negative values of ξ (suction) and to increase slightly for positive values of ξ (blowing) as δ increases. These behaviors are also clear from Figs. 5 and 6.

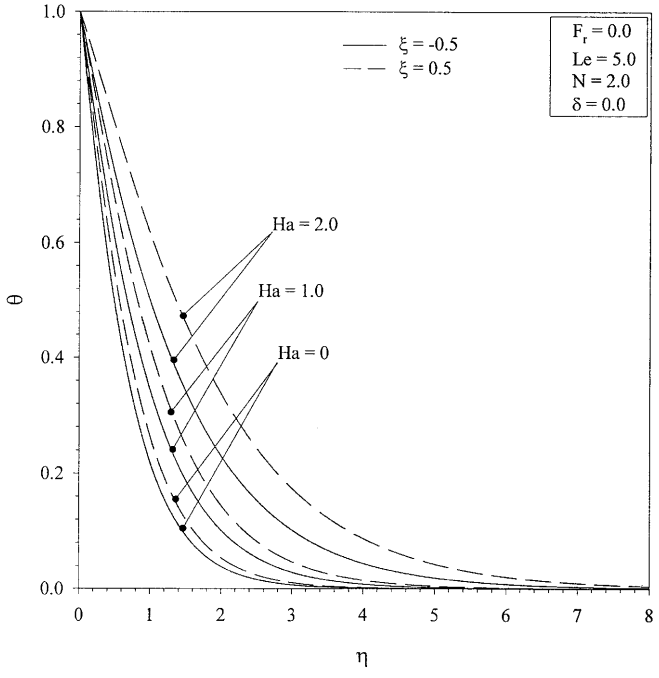

Fig. 2. Effects of Ha on temperature profiles (UWT/UWC)

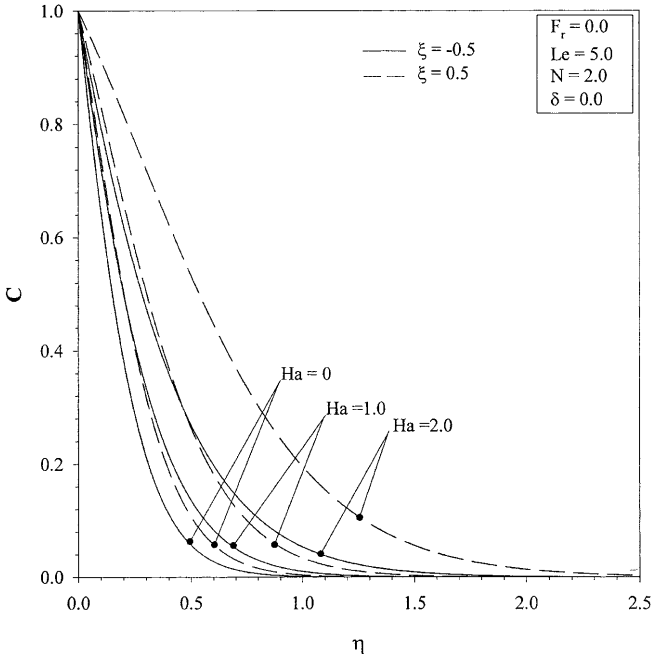

Fig. 3. Effects of Ha on concentration profiles (UWT/UWC)

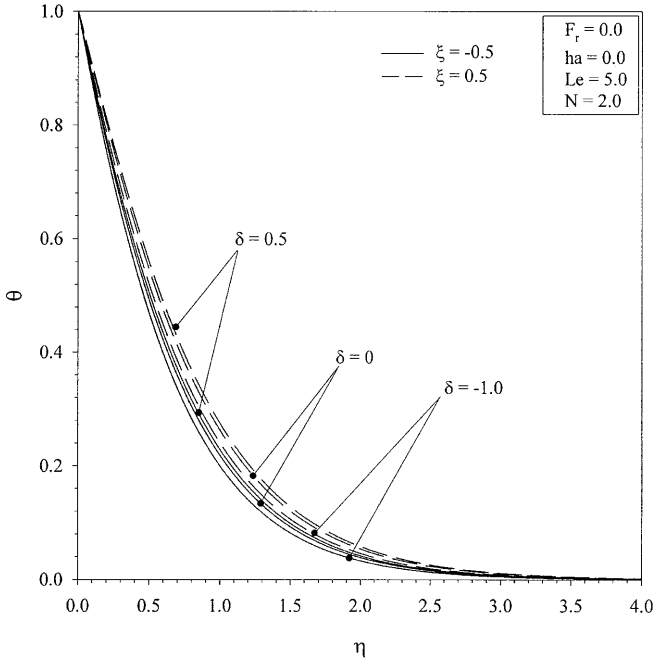

Fig. 4. Effects of δ on temperature profiles (UWT/UWC)

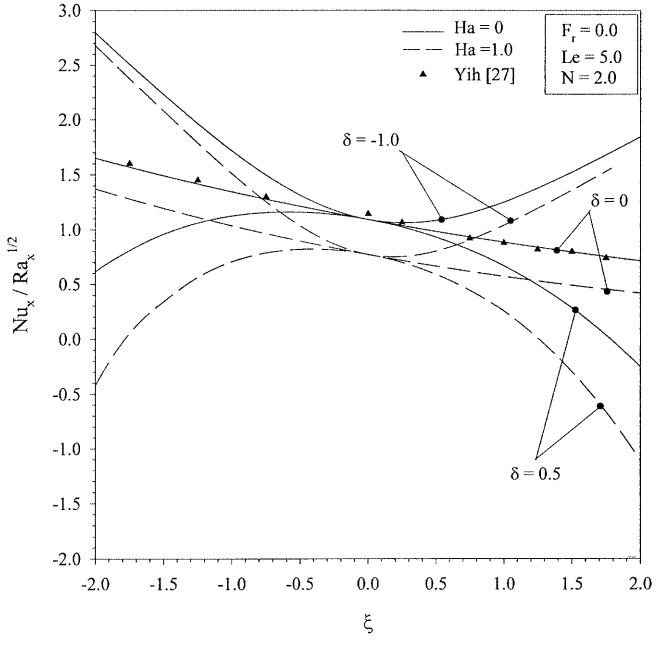

Fig. 5. Effects of Ha and δ on local Nusselt number (UWT/UWC)

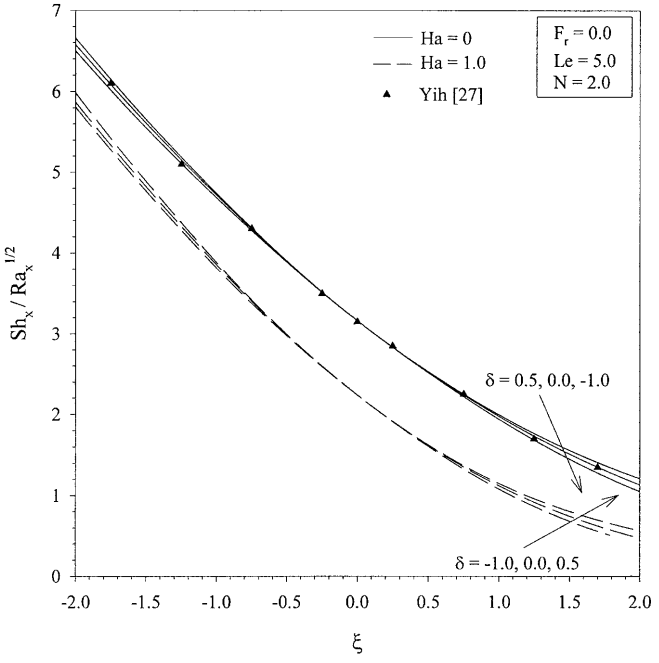

Fig. 6. Effects of Ha and δ on local Sherwood number (UWT/UWC)

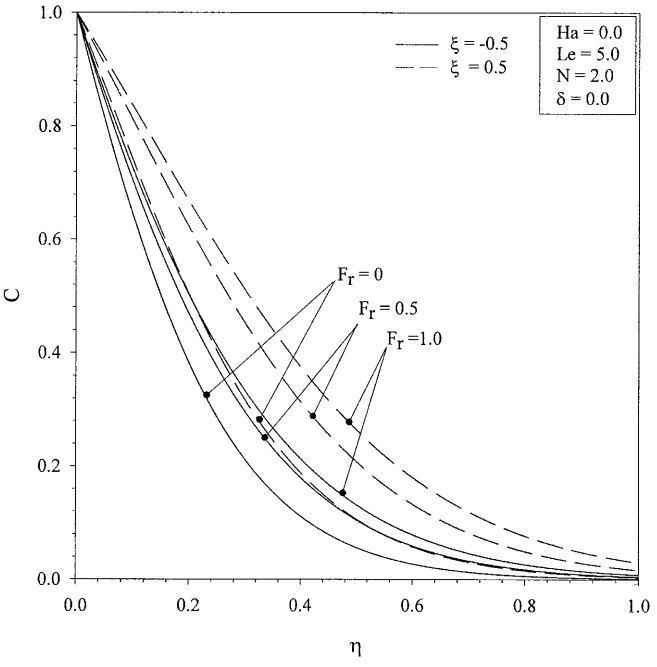

Fig. 8. Effect of F_r on concentration profiles (UWT/UWC)

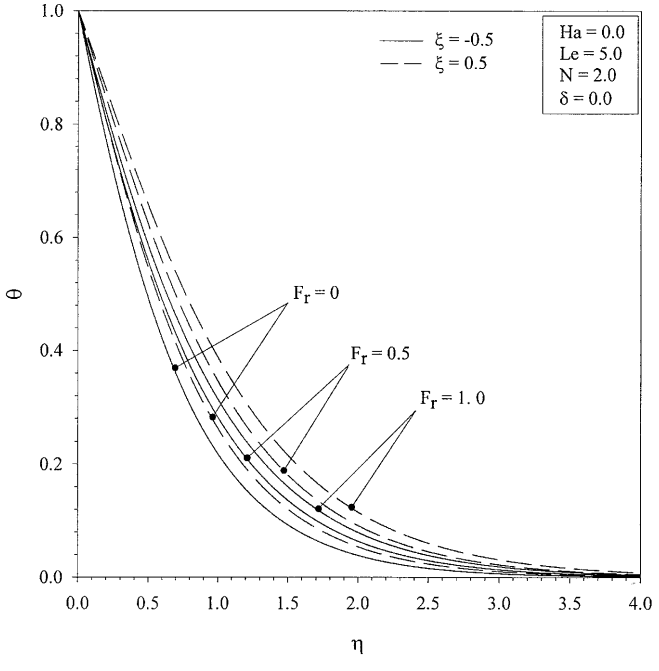

Fig. 7. Effects of F_r on temperature profiles (UWT/UWC)

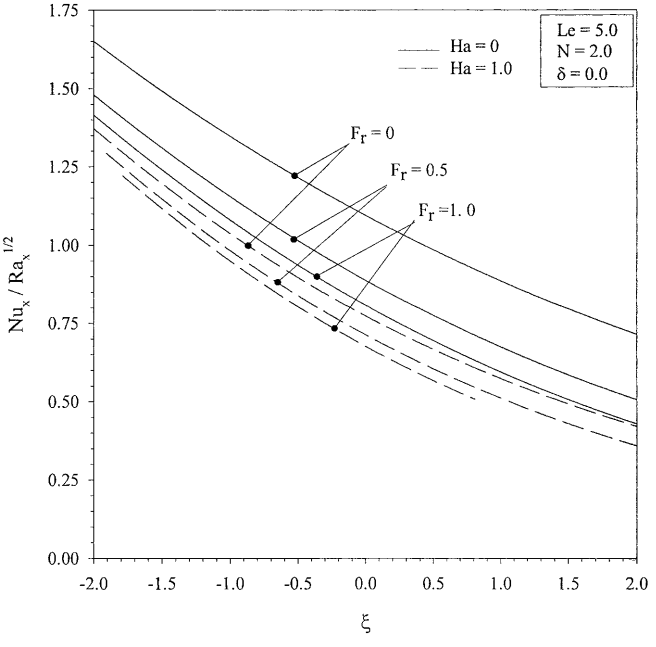

Fig. 9. Effects of F_r and Ha on local Nusselt number (UWT/UWC)

Figures 7 through 8 present the effects of and the porous medium inertia parameter F_r on the temperature and concentration profiles for two values of the suction or injection parameter ξ, respectively. In analogy with the magnetic field, the porous medium inertia effects increase the resistance on the flow. Therefore, similar to magnetic field, the effect of the porous medium inertia parameter F_r is predicted to increase the temperature and concentration values for all values of ξ considered.

In Figs. 9 and 10, the effects of F_r on the local Nusselt and Sherwood numbers for both Ha = 0 and 1.0 and various values of ξ ranging from $\xi = -2.0$ to 2.0 are presented for the (UWT/UWC) case, respectively. In these figures, it is predicted that both the local Nusselt and Sherwood numbers decrease as the porous medium inertia parameter F_r increases for the same reasons as those of the magnetic field.

Finally, Figs. 11 through 14 show the influence of the dimensionless heat generation or absorption coefficient δ on the temperature and concentration profiles as well as

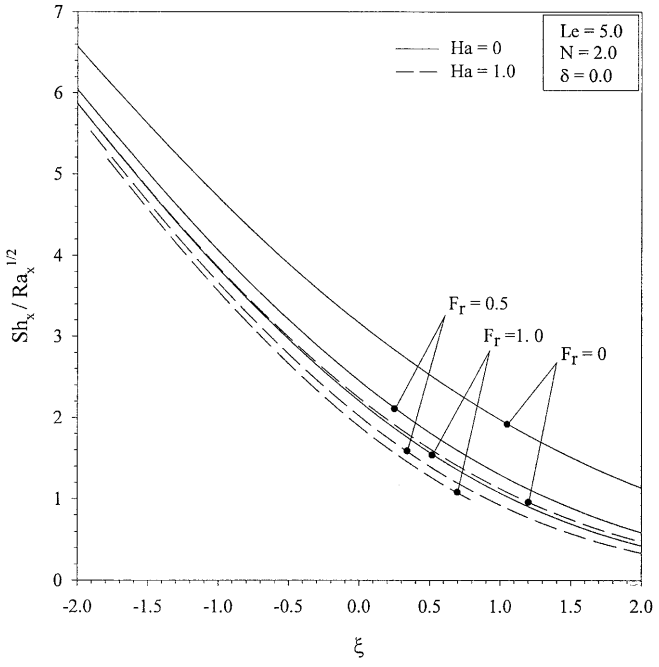

Fig. 10. Effects of F_r and Ha on local Sherwood number (UWT/UWC)

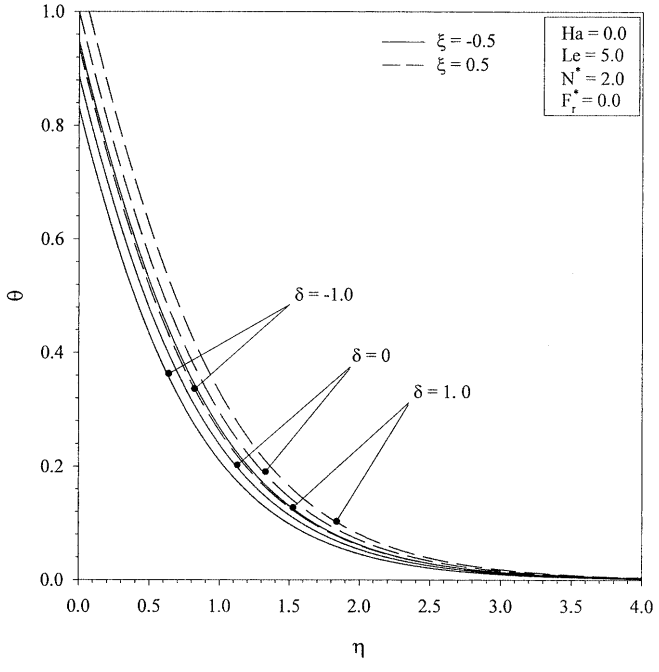

Fig. 11. Effects of δ on temperature profiles (UHF/UMF)

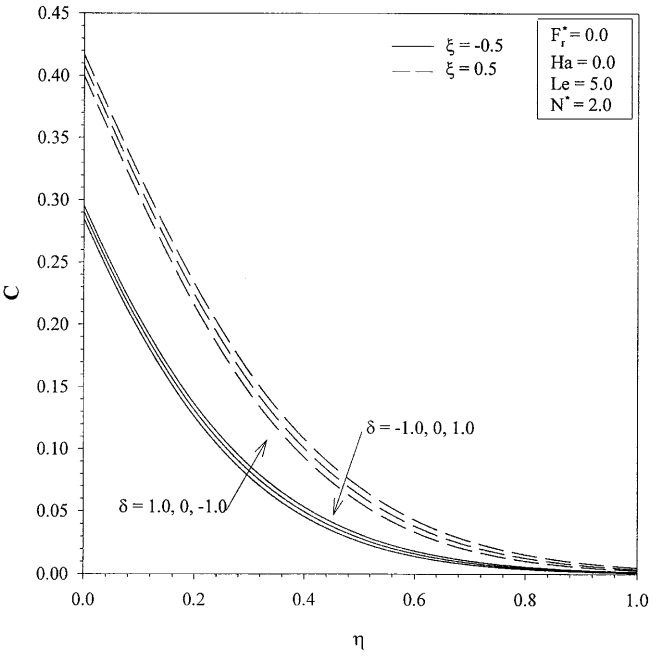

Fig. 12. Effects of δ on concentration profiles (UHF/UMF)

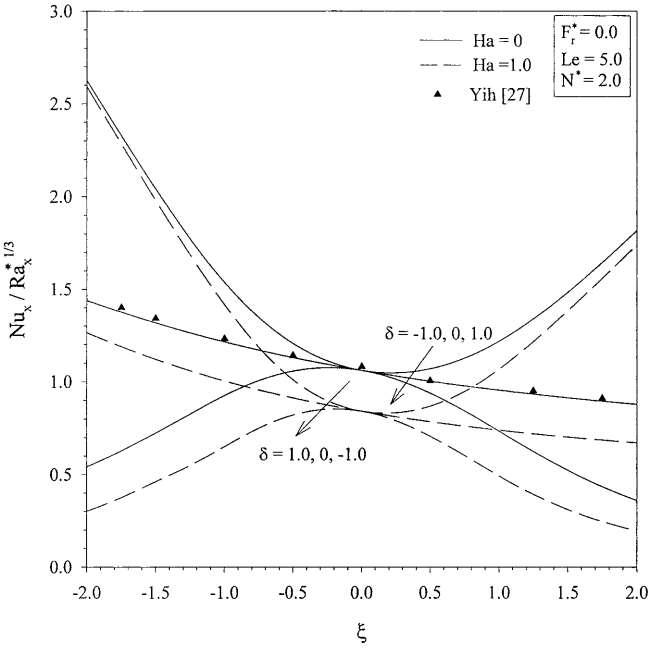

Fig. 13. Effects of Ha and δ on local Nusselt number (UHF/UMF)

the local Nusselt and Sherwood numbers for the (UHF/UMF) case, respectively. As in the (UWT/UWC) case, increasing the heat generation or absorption coefficient δ causes an increase in the fluid temperature and a decrease in the concentration. This is true irregardless of the value of ξ. This is accompanied by an increase in the wall temperature $\theta(\xi, 0)$ and a decrease in the wall concentration $C(\xi, 0)$. This has the direct effect of decreasing the local Nusselt number and increasing the local Sherwood number. These behaviors are clearly depicted in Figs. 11 through 14.

All of the above behaviors can be related to physical processes. For example, in petroleum production, while the presence of a heat source enhances production rates, the wall heat transfer decreases. Furthermore, the presence of porous medium inertia effects requires more energy for constant rates of oil production. Also, the contaminants concentration level in electrically-conducting fluids such as liquid metals tends to increase as a result of the presence of a magnetic field.

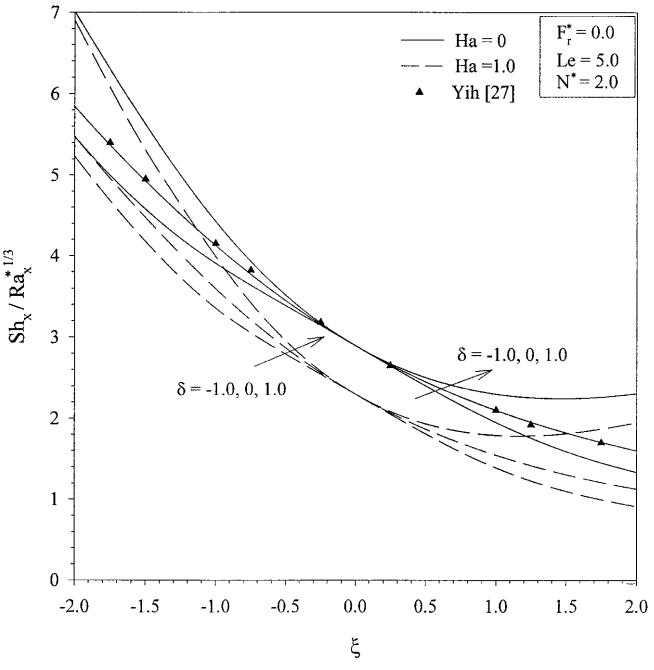

Fig. 14. Effects of Ha and δ on local Sherwood number (UHF/UMF)

5 Conclusion

The problem of combined heat and mass transfer by natural convection from a permeable cone embedded in a uniform porous medium in the presence of porous medium inertia, magnetic field and heat generation or absorption effects was considered. Two thermal and concentration boundary conditions were considered. These conditions were the uniform wall temperature/uniform wall concentration (UWT/UWC) and the uniform wall heat flux/uniform wall mass flux (UHF/UMF). Non-similarity variables were employed to transform the governing equations of both cases. The obtained transformed non-similar equations were solved numerically by an implicit, tri-diagonal finite-difference method. The obtained results were checked against previously published work and were found to be in excellent agreement. Numerical results for the temperature and concentration profiles as well as the local Nusselt and Sherwood numbers were reported graphically. It was found that both the local Nusselt and Sherwood numbers decreased due to increases in either of the Hartmann number or the porous medium inertia parameter for both the (UWT/UWC) and the (UHF/UMF) cases. The heat generation effects were found to decrease the local Nusselt number for both the (UWT/UWC) and the (UHF/UMF) cases. However, the opposite behavior was predicted for the heat absorption effects. Also, in the absence of the heat generation/absorption effects, both the local Nusselt and Sherwood numbers had a decreasing trend with the suction/injection parameter. However, in the presence of heat absorption, the local Nusselt number increased as the fluid suction or blowing amount increased. The opposite behavior was obtained for the heat generation case. These trends were predicted for both the (UWT/UWC) and the (UHF/UMF) cases. It is hoped that the present work be useful for validating more complex studies dealing with heat and mass transfer from cones embedded in porous media.

References

1. **Nield DA; Bejan A** (1999) Convection in Porous Media, 2nd edn. Springer-Verlag, New York
2. **Trevisan OV; Bejan A** (1990) Mass and heat transfer by natural convection in a vertical slot filled with porous medium. Int J Heat Mass Transfer 29: 403–415
3. **Cheng P; Minkowycz WJ** (1977) Free convection about a vertical flat plate embedded in a porous medium with application to heat transfer from a dike. J Geophy 82: 2040–2044
4. **Johnson CH; Cheng P** (1978) Possible similarity solutions for free convection boundary-layers adjacent to flat plates in porous media. Int J Heat Mass Transfer 21: 709–718
5. **Vafai K; Tien CL** (1981) Boundary and inertia effects on flow and heat transfer in porous media. Int J Heat Mass Transfer 24: 195–203
6. **Plumb OA; Huenefeld TC** (1981) Non-Darcy natural-convection from heated surfaces in saturated porous media. Int J Heat Mass Transfer 24: 765–768
7. **Merkin JH** (1979) Free convection boundary layers on axisymmetric and two-dimensional bodies of arbitrary shape in a saturated porous medium. Int J Heat Mass Transfer 22: 1461–1462
8. **Fand RM; Steinberger TE; Cheng P** (1986) Natural convection heat transfer from a horizontal cylinder embedded in a porous medium. Int J Heat Mass Transfer 29: 119–133
9. **Nakayama A; Koyama H** (1987) Free convection heat transfer over a nonisothermal body of arbitrary shape embedded in a fluid-saturated porous medium. ASME J Heat Transfer 109: 125–130
10. **Ingham DB; Pop I** (1987) Natural convection about a heated horizontal cylinder in a porous medium. J Fluid Mech 184: 157–181
11. **Pop I; Kumari M; Nath G** (1992) Free convection about cylinders of elliptic cross section embedded in a porous medium. Int J Eng Sci 30: 35–45
12. **Sparrow EM; Cess RD** (1961) Effects of magnetic field on free convection heat transfer. Int J Heat Mass Transfer 3: 267–274
13. **Gray DD** (1979) The laminar wall plume in a transverse magnetic field. Int Commun Heat Mass Transfer 22: 1155–1158
14. **Michiyoshi I; Takahashi I; Serizawa A** (1976) Natural convection heat transfer from a horizontal cylinder to mercury under magnetic field. Int J Heat Mass Transfer 19: 1021–1029
15. **Fumizawa M** (1980) Natural convection experiment with liquid NaK under transverse magnetic field. J Nuclear Sci Tech 17: 10–17
16. **Riley N** (1964) Magnetohydrodynamics free convection. J Fluid Mech 18: 577–586
17. **Vajravelu K; Hadjinicolaou A** (1993) Heat transfer in a viscous fluid over a stretching sheet with viscous dissipation and internal heat generation. Int Commun Heat Mass Transfer 20: 417–430
18. **Vajravelu K; Nayfeh J** (1992) Hydromagnetic convection at a cone and a wedge. Int Commun Heat Mass Transfer 19: 701–710
19. **Kou HS; Lu KT** (1993) Combined boundary and inertia effects for fully developed mixed convection in a vertical channel embedded in porous media. Int Commun Heat Mass Transfer 20: 333–345
20. **Chamkha AJ** (1996) Non-Darcy hydromagnetic free convection from a cone and a wedge in porous media. Int Commun Heat Mass Transfer 23: 875–887

21. **Bejan A; Khair KR** (1985) Heat and mass transfer by natural convection in a porous medium. Int Commun Heat Mass Transfer 28: 909–918
22. **Jang JY; Chang WJ** (1988) Buoyancy-induced inclined boundary layer flow in a porous medium resulting from combined heat and mass buoyancy effects. Int Commun Heat Mass Transfer 15: 17–30
23. **Lai FC; Kulacki FA** (1991) Non-Darcy mixed convection along a vertical wall in a saturated porous medium. Int J Heat Mass Transfer 113: 252–255
24. **Yucel A** (1990) Natural convection of heat and mass transfer along a vertical cylinder in a porous medium. Int J Heat Mass Transfer 33: 2265–2274
25. **Lai FC; Kulacki FA** (1990) Coupled heat and mass transfer from a sphere buried in an infinite porous medium. Int J Heat Mass Transfer 33: 209–215
26. **Yih KA** (1999) Coupled heat and mass transfer by natural convection adjacent to a permeable horizontal cylinder in a saturated porous medium. Int Commun Heat Mass Transfer 26: 431–440
27. **Yih KA** (1999) Uniform transpiration effect on combined heat and mass transfer by natural convection over a cone in saturated porous media: uniform wall temperature/concentration or heat/mass flux. Int J Heat Mass Transfer 42: 3533–3537
28. **Cramer KR; Pai SI** (1973) Magneto Fluid Dynamics for Engineers and Applied Physicists. McGraw-Hill Book Company, New York
29. **Blottner FG** (1970) Finite-difference methods of solution of the boundary-layer equations. AIAA J 8: 193–205